to dimer interactions. Furthermore, these excited-state interactions provide experimental insight into the superexchange pathways involving different combinations of d orbitals and, in addition, directly relate to the origin of the ground-state spin Hamiltonian parameters.

Acknowledgment. We thank Professor D. S. McClure for informing us of the excited-state vibronic structure exhibited by this system, Professor R. L. Musselman for information on crystal morphology, and Dr. J. J. Girerd for useful discussions. This research is supported by NIH Grant DK31450.

Registry No. Copper acetate pyrazine, 51798-90-4.

Supplementary Material Available: Spin-orbit matrixes for the even and odd parity dimer-state wave functions given in Table IB,C (2 pages). Ordering information is given on any current masthead page.

Complexation of Tin(II) by the Iridium Metallomacrocycle $Ir_2(CO)_2Cl_2(\mu\text{-}Ph_2PCH_2As(Ph)CH_2PPh_2)_2$. A Novel Receptor and Sensor of Tin(II)

Alan L. Balch,* Marilyn M. Olmstead, Douglas E. Oram, Philip E. Reedy, Jr., and Steven H. Reimer

Contribution from the Department of Chemistry, University of California, Davis, California 95616. *Received July 25, 1988*

Abstract: Tin(II) chloride reacts with yellow $Ir_2(CO)_2Cl_2(\mu\text{-dpma})_2$ (dpma is $Ph_2PCH_2As(Ph)CH_2PPh_2$) to yield blue $[Ir_2(SnCl)(CO)_2Cl_2(\mu\text{-dpma})_2]SnCl_3$. The X-ray crystal structure of a derivative, $[Ir_2(SnCl)(CO)_2Cl_2(\mu\text{-dpma})_2][Ir(SnCl_3)_2(CO)(dpma)]$, which crystallizes in the triclinic space group $P\bar{1}$ with a = 16.739 (7) Å, b = 17.030 (7) Å, c = 21.785 (9) Å, α = 79.61 (3)°, β = 75.97 (3)°, γ = 67.78 (3)°, Z = 2 at 130 K, has been determined. Least-squares refinement of 665 parameters using 7363 reflections yielded R = 0.063. The cation consists of the intact metallomacrocycle with the tin symmetrically bound only to the two iridium ions and a chloride (Ir-Sn distances, 2.741 (2) Å, 2.742 (2) Å, Sn-Cl, 2.443 (7) Å, Ir-Sn-Ir angle, 146.1°) in a planar arrangement. The anion consists of an iridium in a trigonal bipyramidal environment with a CO and P as the axial ligands. The dpma acts as a six-membered chelating ligand with the arsenic atom uncoordinated. $[Ir_2(SnCl)(CO)_2Cl_2(\mu\text{-dpma})_2]^+$ has an intense blue color, λ_{max} = 588 (ϵ = 77000) and luminescence at 645 nm, that makes it a sensitive sensor for tin(II). $Ir_2(CO)_2Cl_2(\mu\text{-dpma})_2$ is capable of selectively extracting tin(II) from an aqueous solution containing Sn(II) and other metal ions and also is capable of transporting Sn(II) from one aqueous phase through dichloromethane to a second aqueous phase. The bonding in the IrSnIr chain is discussed in the context of other nearly linear trinuclear complexes.

The metallomacrocycle $Ir_2(CO)_2Cl_2(\mu\text{-dpma})_2$, **1** (dpma is bis(diphenylphosphinomethyl)phenylarsine), is capable of binding

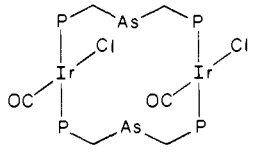

1

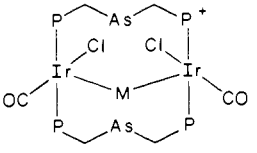

2a, M = Tl
b, M = Pb(NO$_3$)

a variety of heavy transition-metal ions through the formation of bonds to the arsenic, iridium, chloride, and/or carbon monoxide parts of **1**.[1] Examples of complexes with transition-metal ions, palladium(II),[2] rhodium(I),[3] iridium(I),[3] copper(I),[4] silver(I),[4,5] gold(III), and gold(I),[6,7] incorporated into **1** have been prepared and structurally characterized by X-ray crystallography.

Recently, we have discovered that **1** is also capable of binding main group ions with an s^2 electronic configuration. A communication describing the intensely colored, luminescent thallium(I) and lead(II) complexes **2** has been published.[8] In these novel materials, the thallium(I) and lead(II) ions are bound only by the two iridium ions of **1**; no bonds to chloride or arsenic are present. This is particularly remarkable since, as we point out in ref 8, the lower oxidation states of these metals, thallium(I) and lead(II), have only been infrequently found to engage in bonding to transition-metal ions.

Here we describe the interactions of **1** with another s^2 ion, tin(II). The interactions of tin(II) chloride with transition metals are well known.[9] Generally, with platinum metal halide complexes, insertion into M-Cl bonds can be anticipated with the formation of M-$SnCl_3$ units as the outcome. That is not the case with **1**.

Results

Synthesis and Characterization of the Complexes. The first of the series of iridium-tin complexes was prepared by treating a dichloromethane solution of $Ir_2(CO)_2Cl_2(\mu\text{-dpma})_2$, **1**, with an excess of $SnCl_2\cdot 2H_2O$ in methanol. The initially yellow solution

(1) Balch, A. L. *Pure Appl. Chem.* **1988**, *60*, 555.
(2) Balch, A. L.; Fossett, L. A.; Olmstead, M. M.; Oram, D. E.; Reedy, P. E., Jr. *J. Am. Chem. Soc.* **1985**, *107*, 5272.
(3) Balch, A. L.; Fossett, L. A.; Olmstead, M. M.; Reedy, P. E., Jr. *Organometallics* **1986**, *5*, 1929.
(4) Balch, A. L.; Olmstead, M. M.; Neve, F.; Ghedini, M. *New J. Chem.* **1988**, *12*, 529.
(5) Balch, A. L.; Ghedini, M.; Oram, D. E.; Reedy, P. E., Jr. *Inorg. Chem.* **1987**, *26*, 1223.
(6) Balch, A. L.; Oram, D. E.; Reedy, P. E., Jr. *Inorg. Chem.* **1987**, *26*, 1836.
(7) Balch, A. L.; Nagle, J. K.; Oram, D. E.; Reedy, P. E., Jr. *J. Am. Chem. Soc.* **1988**, *110*, 454.
(8) Balch, A. L.; Nagle, J. K.; Olmstead, M. M.; Reedy, P. E., Jr. *J. Am. Chem. Soc.* **1987**, *109*, 4123.
(9) Young, J. F.; Gillard, R. D.; Wilkinson, G. *J. Chem. Soc.* **1964**, 5176. Anderson, G. K.; Clark, H. C.; Davies, J. A. *Inorg. Chem.* **1983**, *22*, 427, 434. Young, J. F. *Adv. Inorg. Chem. Radiochem.* **1968**, *11*, 91. Zubieta, J. A.; Zuckerman, J. J. *Prog. Inorg. Chem.* **1978**, *24*, 251. Olmstead, M. M.; Benner, L. S.; Hope, H.; Balch, A. L. *Inorg. Chim. Acta* **1979**, *32*, 193.

0002-7863/89/1511-4021$01.50/0

of **1** immediately turned a very intense blue color upon addition of the $SnCl_2$. Addition of methanol to this solution causes the product $[Ir_2(SnCl)(CO)_2Cl_2(\mu\text{-dpma})_2][SnCl_3]$, **3**, to precipitate

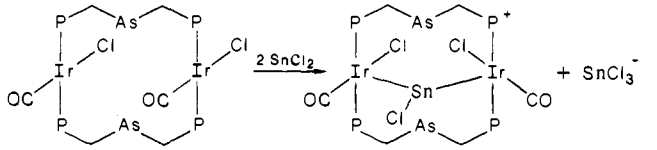

1 3 (1)

as blue needles in good yield. The ^{31}P NMR spectrum of the complex shows only a single sharp reasonance at 26.9 ppm, indicating that the two IrP_2 environments are equivalent in solution. (For comparison, **1** has a singlet at 18.6 ppm in the ^{31}P NMR spectrum.) The infrared spectrum exhibits two carbonyl stretches at 1987 and 1974 cm^{-1}, which are normal for carbonyl ligands bound to Ir(I) and indicates that the two Ir(I) ions in **1** have not been oxidized or reduced in the reaction.[10] To determine the precise stoichiometry of the reaction, a solution of **1** was titrated with $SnCl_2 \cdot 2H_2O$, and the conversion to **3** was monitored by ^{31}P NMR. The results indicate that 2 equiv of tin are required to cleanly convert the starting material to product. The consumption of 2 equiv of tin in the reaction is due to formation of an $SnCl_3^-$ anion as shown in eq 1. The addition of only 1 equiv of $SnCl_2 \cdot 2H_2O$ results in the formation of a 1:1 mixture of **1** and **3**. Elemental analysis of the complex confirms the presence of the $SnCl_3^-$ anion. In dichloromethane solution **2** acts as a 1:1 electrolyte with $\Lambda_M = 49$ ohm^{-1} mol^{-1} cm^2. For comparison, $[Rh_2Au(CO)_2Cl_2(\mu\text{-dpma})_2][BPh_4]$ and $[Ir_2Au(CO)_2Br_2(\mu\text{-dpma})_2]BPh_4$ have molar conductivities of 47 and 49 ohm^{-1} mol^{-1} cm^2.

Treatment of **3** with a methanol solution of sodium tetraphenylborate results in formation of the tetraphenylborate salt $[Ir_2(SnCl)(CO)_2Cl_2(\mu\text{-dpma})_2][BPh_4]$, **4**. Spectroscopic studies show that the cation in both salts is identical. The tetraphenylborate salt crystallizes as very fine, fiber-like needles, while the $SnCl_3^-$ salt forms more dense three-dimensional crystals. Elemental analysis confirms that the $SnCl_3^-$ anion has been replaced with BPh_4^-.

In order to examine the effect of the anion on the reactivity of the tin(II) compounds, the behavior of tin(II) sulfate was examined. Treatment of a dichloromethane solution of **1** with a slurry of $SnSO_4$ in methanol results in a deep blue solution from which bright blue crystals were isolated upon addition of methanol. The spectroscopic properties of this complex, $[Ir_2(SnSO_4)(CO)_2Cl_2(\mu\text{-dpma})_2]$, **5**, are slightly different than those observed for **3** and **4**. The carbonyl stretching frequency in the infrared spectrum is approximately 10 cm^{-1} higher in energy than the average of the two observed in **3** and **4**. In addition, both the electronic absorption spectra and ^{31}P NMR spectra show small, although significant deviations. Although it was anticipated that this complex would contain a dication, $[Ir_2Sn(CO)_2Cl_2(\mu\text{-dpma})_2]^{2+}$, and a sulfate dianion, a dichloromethane solution of the complex was found to be nonconducting. This indicates that the sulfate ion is not dissociated in solution, leading to a formulation for the neutral complex as $[Ir_2(SnSO_4)(CO)_2Cl_2(\mu\text{-dpma})_2]$, **5**.

The X-ray Crystal Structure of $[Ir_2(SnCl)(CO)_2Cl_2(\mu\text{-dpma})_2][Ir(CO)(SnCl_3)_2(dpma)] \cdot 2.25CH_2Cl_2$. Due to the difficulty in growing crystals of suitable quality for an X-ray diffraction study from solutions of **3**, a methanolic solution of $SnCl_2 \cdot 2H_2O$ and $NaBPh_4$ was allowed to diffuse slowly into a dichloromethane solution of **1**. Initially, only small needles formed, but after 6 weeks large well-formed crystals had grown which were suitable for a structure determination. The complex consists of a cation and anion which are shown in Figures 1 and 2. Atomic positional parameters are given in Table I, and selected interatomic distances and angles are presented in Tables II and III. It is clear that during the crystal-growing process, the anion was created from

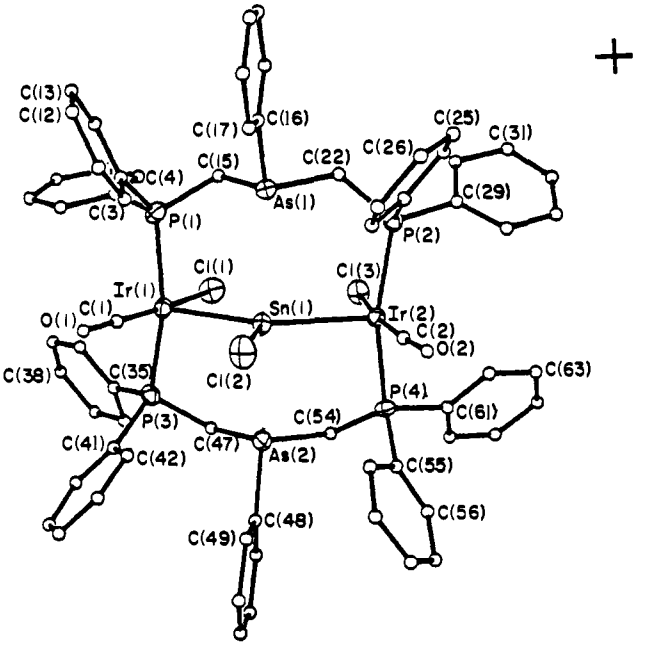

Figure 1. A perspective view of $[Ir_2(SnCl)(CO)_2Cl_2(\mu\text{-dpma})_2]^+$ showing 50% thermal ellipsoid contours for heavy atoms and uniform arbitrarily sized circles for carbon atoms.

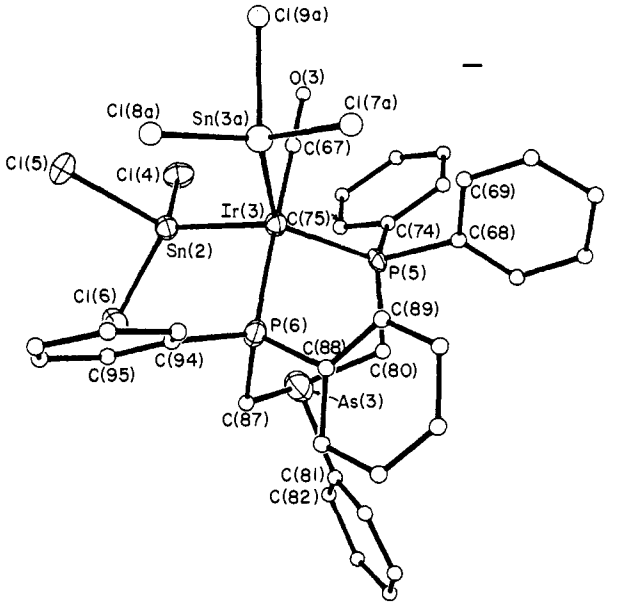

Figure 2. A perspective view of $[Ir(CO)(SnCl_3)_2(dpma)]^-$. For the disordered $SnCl_3^-$ involving Sn(3a), only the positions of the major form are shown.

the original metallomacrocycle **1**. However, the crystalline sample, when dissolved in dichloromethane, gave the 588-nm absorption band characteristic of **3** (vide infra).

A view of the cation is shown in Figure 1. It consists of the intact metallomacrocycle **1** with a $SnCl^+$ group bound to the central cavity through the two iridium ions. While the cation has no crystallographically imposed symmetry, it does have approximate C_{2v} symmetry with the C_2 axis coinciding with the Sn–Cl bond. The two Sn–Ir distances (2.741 (2) and 2.742 (2) Å) are nearly identical. These distances are longer than the range of Ir–Sn distances (2.57–2.64 Å) seen in compounds where an $SnCl_3^-$ ligand is present.[11,12] The Sn(1)–Cl(2) distance (2.443 (7) Å)

(10) Vaska, L. *Acc. Chem. Res.* **1968**, *1*, 335.

(11) Porta, P.; Powell, M. H.; Mawby, R. J.; Vananzi, L. M. *J. Chem. Soc.* **1967**, 455.

(12) Balch, A. L.; Waggoner, K. M.; Olmstead, M. M. *Inorg. Chem.* **1988**, *27*, 4511.

Table I. Atomic Coordinates ($\times 10^4$) and Isotropic Thermal Parameters ($Å^2 \times 10^3$) for $[Ir_2(SnCl)(CO)_2Cl_2(\mu\text{-dpma})_2][Ir(CO)(SnCl_3)_2(dpma)]$

	x	y	z	U		x	y	z	U
Ir(1)	126 (1)	2139 (1)	3900 (1)	22 (1)[a]	C(56)	2455 (18)	5680 (18)	2625 (13)	45 (8)
Ir(2)	61 (1)	4936 (1)	2403 (1)	20 (1)[a]	C(57)	2586 (19)	6195 (19)	3029 (14)	53 (9)
Sn(1)	−81 (1)	3802 (1)	3454 (1)	22 (1)[a]	C(58)	2046 (19)	6400 (18)	3597 (13)	45 (8)
As(1)	−1897 (2)	3965 (2)	3144 (1)	25 (1)[a]	C(59)	1372 (17)	6094 (16)	3813 (12)	33 (7)
As(2)	1855 (2)	3382 (2)	3492 (1)	25 (1)[a]	C(60)	1171 (17)	5645 (16)	3438 (12)	33 (7)
P(1)	−1182 (4)	2110 (4)	3730 (3)	28 (3)[a]	C(61)	1956 (16)	5109 (15)	1539 (11)	29 (6)
P(2)	−1303 (4)	5258 (4)	2123 (3)	24 (3)[a]	C(62)	1379 (18)	5736 (7)	1202 (13)	41 (7)
P(3)	1584 (4)	1646 (4)	4036 (3)	25 (3)[a]	C(63)	1686 (18)	6015 (16)	578 (12)	38 (7)
P(4)	1528 (4)	4771 (4)	2361 (3)	23 (3)[a]	C(64)	2550 (17)	5645 (16)	284 (12)	33 (7)
Cl(1)	730 (4)	1779 (4)	2837 (3)	35 (3)[a]	C(65)	3111 (19)	5012 (18)	628 (14)	49 (8)
Cl(2)	−678 (5)	4624 (4)	4376 (3)	41 (3)[a]	C(66)	2831 (19)	4713 (18)	1244 (13)	48 (8)
Cl(3)	621 (4)	3789 (4)	1756 (3)	31 (3)[a]	Ir(3)	6792 (1)	1394 (1)	1478 (1)	22 (1)[a]
O(1)	−584 (10)	2360 (10)	5266 (7)	28 (4)	Sn(2)	5967 (1)	3009 (1)	1328 (1)	24 (1)[a]
O(2)	−581 (11)	6583 (10)	2959 (7)	32 (4)	Sn(3A)	6051 (2)	779 (2)	2541 (1)	30
C(1)	−318 (15)	2304 (15)	4733 (11)	25 (6)	Sn(3B)	5780 (4)	918 (3)	2444 (2)	30
C(2)	−337 (17)	5913 (17)	2776 (12)	36 (7)	As(3)	7439 (2)	1779 (2)	−311 (1)	42 (1)[a]
C(3)	−958 (17)	1000 (16)	3644 (12)	35 (7)	P(5)	8156 (4)	717 (4)	903 (3)	21 (3)[a]
C(4)	−746 (19)	708 (18)	3039 '13)	46 (8)	P(6)	6096 (4)	1098 (4)	783 (3)	27 (3)[a]
C(5)	−504 (21)	−164 (20)	2994 (15)	63 (10)	Cl(4)	6815 (4)	3844 (4)	1425 (3)	36 (3)[a]
C(6)	−480 (20)	−716 (19)	3554 (14)	53 (9)	Cl(5)	4681 (4)	3750 (4)	2065 (3)	40 (3)[a]
C(7)	−659 (20)	−459 (19)	4171 (14)	54 (9)	Cl(6)	5490 (4)	3834 (4)	387 (3)	35 (3)[a]
C(8)	−912 (18)	449 (17)	4213 (12)	40 (7)	Cl(7A)	6400 (7)	−703 (7)	2834 (5)	40
C(9)	−2200 (16)	2425 (16)	4350 (11)	31 (7)	Cl(8A)	4504 (8)	1140 (8)	2901 (5)	40
C(10)	−2376 (21)	3044 (19)	4727 (15)	58 (9)	Cl(9A)	6353 (8)	1073 (7)	3446 (5)	40
C(11)	−3193 (20)	3324 (18)	5168 (14)	50 (8)	Cl(7B)	5748 (12)	−508 (11)	2703 (8)	40
C(12)	−3811 (18)	2941 (18)	5176 (13)	44 (8)	Cl(8B)	4225 (12)	1674 (12)	2651 (9)	40
C(13)	−3651 (21)	2321 (20)	4780 (15)	61 (9)	Cl(9B)	5910 (24)	927 (22)	3491 (16)	40
C(14)	−2828 (21)	2017 (20)	4353 (15)	62 (9)	Cl(9C)	5904 (26)	1373 (24)	3437 (18)	40
C(15)	−1538 (17)	2731 (16)	3024 (12)	36 (7)	O(3)	7721 (14)	1786 (13)	2349 (10)	65 (6)
C(16)	−3179 (17)	4388 (16)	3394 (12)	35 (7)	C(67)	7347 (18)	1612 (17)	1999 (13)	44 (8)
C(17)	−3553 (18)	4880 (18)	3897 (13)	43 (8)	C(68)	8757 (15)	−388 (15)	1167 (11)	24 (6)
C(18)	−4494 (21)	5186 (20)	4076 (15)	62 (9)	C(69)	8580 (16)	−676 (15)	1814 (11)	24 (6)
C(19)	−5000 (23)	5034 (22)	3734 (16)	76 (11)	C(70)	9086 (18)	−1478 (17)	2024 (12)	38 (7)
C(20)	−4664 (22)	4556 (21)	3254 (16)	70 (10)	C(71)	9789 (18)	−2065 (17)	1631 (13)	43 (8)
C(21)	−3691 (20)	4231 (19)	3042 (14)	54 (9)	C(72)	9935 (16)	−1768 (15)	988 (11)	29 (6)
C(22)	−1680 (16)	4362 (15)	2206 (11)	28 (6)	C(73)	9431 (18)	−916 (17)	750 (12)	39 (7)
C(23)	−2219 (15)	6079 (14)	2553 (11)	23 (6)	C(74)	8910 (15)	1249 (14)	922 (10)	21 (6)
C(24)	−2885 (19)	6629 (18)	2235 (13)	46 (8)	C(75)	8697 (16)	2127 (15)	750 (11)	29 (6)
C(25)	−3567 (20)	7251 (19)	2579 (15)	58 (9)	C(76)	9185 (19)	2601 (18)	838 (13)	46 (8)
C(26)	−3679 (21)	7317 (20)	3215 (15)	65 (10)	C(77)	9966 (18)	2115 (17)	1108 (13)	44 (8)
C(27)	−2979 (18)	6729 (7)	3527 (13)	42 (8)	C(78)	10188 (18)	1260 (17)	1264 (12)	41 (7)
C(28)	−2278 (15)	6133 (14)	3185 (10)	21 (6)	C(79)	9691 (16)	801 (15)	1175 (11)	26 (6)
C(29)	−1231 (16)	5672 (15)	1298 (11)	27 (6)	C(80)	8195 (17)	690 (16)	57 (12)	36 (7)
C(30)	−1379 (20)	5252 (18)	846 (14)	52 (9)	C(81)	7744 (20)	1349 (19)	−1179 (14)	52 (8)
C(31)	−1308 (19)	5628 (19)	178 (14)	50 (8)	C(82)	8082 (22)	1892 (21)	−1635 (16)	65 (10)
C(32)	−1024 (19)	6284 (18)	19 (13)	48 (8)	C(83)	8358 (25)	1587 (25)	−2290 (18)	87 (12)
C(33)	−902 (19)	6694 (18)	443 (14)	50 (8)	C(84)	8309 (25)	806 (25)	−2347 (18)	87 (12)
C(34)	−1000 (17)	6388 (16)	1107 (12)	33 (7)	C(85)	7962 (21)	322 (20)	−1851 (15)	59 (9)
C(35)	2081 (16)	508 (15)	3937 (11)	28 (6)	C(86)	7675 (21)	627 (21)	−1270 (15)	60 (9)
C(36)	1519 (16)	54 (15)	4096 (11)	29 (6)	C(87)	6292 (17)	1614 (16)	−39 (12)	36 (7)
C(37)	1886 (19)	−847 (18)	4031 (13)	47 (8)	C(88)	6413 (18)	−47 (17)	676 (13)	43 (8)
C(38)	2759 (19)	−1270 (18)	3771 (13)	47 (8)	C(89)	6897 (17)	−665 (17)	1092 (12)	36 (7)
C(39)	3299 (23)	−750 (22)	3621 (17)	77 (11)	C(90)	7129 (19)	−1522 (18)	1014 (13)	47 (8)
C(40)	2982 (19)	137 (18)	3677 (14)	52 (8)	C(91)	6840 (19)	−1742 (19)	518 (14)	50 (8)
C(41)	1788 (18)	1739 (17)	4807 (12)	40 (7)	C(92)	6360 (22)	−1100 (21)	98 (16)	67 (10)
C(42)	1311 (16)	2531 (15)	5071 (11)	28 (6)	C(93)	6128 (19)	−234 (18)	177 (14)	52 (8)
C(43)	1450 (17)	2612 (16)	5648 (12)	37 (7)	C(94)	4876 (17)	1411 (16)	1024 (12)	32 (7)
C(44)	2059 (20)	1984 (19)	5962 (14)	57 (9)	C(95)	4331 (19)	2213 (18)	861 (13)	44 (8)
C(45)	2553 (20)	1216 (19)	5683 (14)	53 (9)	C(96)	3413 (22)	2460 (20)	1080 (15)	60 (9)
C(46)	2415 (16)	1083 (15)	5115 (11)	29 (6)	C(97)	3037 (21)	1868 (20)	1453 (15)	60 (9)
C(47)	2293 (16)	2123 (15)	3469 (11)	25 (6)	C(98)	3636 (25)	1048 (23)	1591 (17)	76 (11)
C(48)	2688 (19)	3536 (17)	3916 (13)	42 (8)	C(99)	4546 (20)	767 (18)	1370 (13)	47 (8)
C(49)	2305 (18)	4028 (17)	4421 (12)	37 (7)	Cl(10)	5582 (7)	2806 (7)	7329 (5)	92 (6)[a]
C(50)	2887 (20)	4139 (19)	4761 (14)	54 (9)	Cl(11)	5361 (9)	1476 (8)	8345 (8)	158 (10)[a]
C(51)	3767 (26)	3734 (25)	4581 (19)	92 (13)	Cl(12)	6019 (9)	3548 (6)	8678 (4)	79 (5)[a]
C(52)	4143 (21)	3261 (20)	4075 (15)	61 (9)	Cl(13)	4225 (7)	3631 (6)	9138 (5)	88 (6)[a]
C(53)	3616 (21)	3104 (20)	3719 (15)	64 (10)	Cl(14)	5188 (16)	547 (15)	5317 (11)	111 (8)
C(54)	2274 (15)	3710 (15)	2576 (11)	24 (6)	C(100)	4919 (21)	4204 (20)	8780 (15)	64 (10)
C(55)	1710 (16)	5446 (15)	2850 (11)	29 (6)	C(101)	6108 (22)	1886 (21)	7844 (16)	67 (10)

[a] Equivalent isotropic U defined as one third of the trace of the orthogonalized U_{ij} tensor.

is just slightly longer than the range of Sn–Cl distances (2.36–2.42 Å) seen in Ir–$SnCl_3$ complexes.[11,12] The coordination about tin is planar with the sum of the two IrSnCl angles and the IrSnIr angle being 360°. The Ir–Sn–Ir angle (146.1 (1)°) is, however, larger than the two nearly identical IrSnCl angles (107.0 (2), 106.9 (2)°). The tin ion is not bound to the arsenic atoms of the dpma backbone. Tin(II)–arsenic bonding is rare: only one structurally characterized example, a disordered one, is available for comparison. In $\{Sn(NO_3)(Ph_3As)(Ph_3Sn)\}_2$ where the Ph_3As and Ph_3Sn^- groups exchange locations, the Sn(II)–As (and Sn(II)–Sn)

Table II. Selected Interatomic Distances (Å)

	$[Ir_2(SnCl)(CO)_2Cl_2(\mu\text{-dpma})_2]^+$		
Ir(1)–Sn(1)	2.741 (2)	Ir(2)–Sn(1)	2.742 (2)
Ir(1)–P(1)	2.327 (9)	Ir(2)–P(2)	2.345 (8)
Ir(1)–P(3)	2.337 (7)	Ir(2)–P(4)	2.344 (7)
Ir(1)–Cl(1)	2.381 (6)	Ir(2)–Cl(3)	2.377 (7)
Ir(1)–C(1)	1.82 (2)	Ir(2)–C(2)	1.81 (3)
C(1)–O(1)	1.15 (3)	C(2)–O(2)	1.17 (3)
Sn(1)–Cl(2)	2.443 (7)	Ir(1)···Ir(2)	5.245 (1)
Sn(1)···As(1)	3.173 (5)	Sn(1)···As(2)	3.062 (5)
	$[Ir(SnCl_3)_2(CO)(dpma)]^-$		
Ir(3)–Sn(2)	2.569 (2)	Sn(2)–Cl(4)	2.423 (9)
Ir(3)–Sn(3A)	2.592 (3)	Sn(2)–Cl(5)	2.409 (6)
Ir(3)–S(3B)	2.579 (5)	Sn(2)–Cl(6)	2.391 (7)
Ir(3)–P(5)	2.292 (6)	Sn(3A)–Cl(7A)	2.368 (12)
Ir(3)–P(6)	2.341 (9)	Sn(3A)–Cl(8A)	2.384 (12)
Ir(3)–C(67)	1.79 (3)	Sn(3A)–Cl(9A)	2.329 (15)
C(67)–O(3)	1.23 (4)	Ir(3)···As(3)	3.789 (5)

Table III. Selected Interatomic Angles for $[Ir_2(SnCl)(CO)_2Cl_2(\mu\text{-dpma})_2][Ir(CO)(SnCl_3)_2(dpma)]$

	$[Ir_2(SnCl)(CO)_2Cl_2(\mu\text{-dpma})_2]^+$		
Ir(1)–Sn(1)–Cl(2)	107.0 (2)	Ir(1)–Sn(1)–Ir(2)	146.1 (1)
Ir(2)–Sn(1)–Cl(2)	106.9 (2)		
P(1)–Ir(1)–P(3)	159.3 (3)	P(2)–Ir(2)–P(4)	162.7 (2)
Cl(1)–Ir(1)–C(1)	174.4 (8)	Cl(3)–Ir(2)–C(2)	170.8 (8)
Sn(1)–Ir(1)–P(1)	99.0 (2)	Sn(1)–Ir(2)–P(2)	99.7 (2)
Sn(1)–Ir(1)–P(3)	99.8 (2)	Sn(1)–Ir(2)–P(4)	96.6 (2)
Sn(1)–Ir(1)–Cl(1)	88.2 (2)	Sn(1)–Ir(2)–Cl(3)	89.1 (1)
Sn(1)–Ir(1)–C(1)	97.4 (8)	Sn(1)–Ir(2)–C(2)	100.0 (8)
P(1)–Ir(1)–Cl(1)	86.3 (3)	P(2)–Ir(2)–Cl(3)	87.4 (2)
P(1)–Ir(1)–C(1)	92.9 (9)	P(2)–Ir(2)–C(2)	91.2 (10)
P(3)–Ir(1)–Cl(1)	85.6 (2)	P(4)–Ir(2)–Cl(3)	86.9 (3)
P(3)–Ir(1)–C(1)	93.4 (8)	P(4)–Ir(2)–C(2)	91.8 (10)
	$[Ir(SnCl_3)_2(CO)(dpma)]^-$		
P(6)–Ir(3)–C(67)	178.8 (9)	P(6)–Ir(3)–Sn(2)	93.4 (2)
Sn(2)–Ir(3)–P(5)	123.5 (2)	P(6)–Ir(3)–Sn(3A)	99.1 (2)
Sn(2)–Ir(3)–Sn(3A)	108.7 (1)	P(6)–Ir(3)–P(5)	91.8 (2)
Sn(3A)–Ir(3)–P(5)	125.8 (2)	C(67)–Ir(3)–Sn(2)	87.2 (8)
		C(67)–Ir(3)–Sn(3A)	81.7 (9)
Ir(3)–C(67)–O(3)	178.0 (2)	C(67)–Ir(3)–P(5)	87.1 (8)
Ir(3)–Sn(2)–Cl(4)	113.2 (2)	Ir(3)–Sn(3A)–Cl(7A)	122.6 (3)
Ir(3)–Sn(2)–Cl(5)	123.1 (2)	Ir(3)–Sn(3A)–Cl(8A)	125.0 (3)
Ir(3)–Sn(2)–Cl(6)	127.3 (2)	Ir(3)–Sn(3A)–Cl(9A)	114.6 (4)
Cl(4)–Sn(2)–Cl(5)	94.9 (3)	Cl(7A)–Sn(3A)–Cl(8A)	95.4 (4)
Cl(4)–Sn(2)–Cl(6)	94.5 (3)	Cl(7A)–Sn(3A)–Cl(9A)	95.9 (4)
Cl(5)–Sn(2)–Cl(6)	96.2 (2)	Cl(8A)–Sn(3A)–Cl(9A)	97.1 (4)

distance is 2.521 (4) Å.[13] In $[Ir_2(SnCl)(CO)_2Cl_2(\mu\text{-dpma})_2]^+$ the Sn···As separations are 3.062 (5) and 3.173 (5) Å.

The iridium ions have retained the $P_2(CO)Cl$ coordination found in **1**. Because of the binding to tin, the two P–Ir–P angles (159.3 (3), 162.7 (2)°) are bent inward. Other aspects of the iridium coordination are similar to those found in other Vaska's type complexes.[14,15]

It is informative to compare the tin binding in $[Ir_2(SnCl)(CO)_2Cl_2(\mu\text{-dpma})_2]^+$ to the silver coordination in the related adduct $Ir_2(AgCl)(CO)_2Cl_2(\mu\text{-dpma})_2$. Tin and silver differ in atomic number by only three and are expected to have very similar sizes.

The structure of $Ir_2Ag(CO)_2Cl_3(\mu\text{-dpma})_2$ has been determined by X-ray crystallography and found to be nearly identical with that published for $Rh_2Ag(CO)_2Cl_3(\mu\text{-dpma})_2$.[5] Details are given in the Supplementary Material. Figure 3 shows a perspective view of the molecule, and Figure 4 compares aspects of the structures of the tin and silver complexes. In contrast to the tin adduct, the silver adduct has the silver bonded to the metallomacrocycle through the two arsenic atoms. The consequences of these differences are seen in Figure 4. While both structures have the same basic metallomacrocyclic structure, the tin complex has the two iridium ions bent inward to bind the tin and the two arsenic atoms relatively far away. In contrast, the silver complex has the two iridium ions spread further apart, while the two arsenic atoms are pulled toward the silver ion. Notice that the As–Ag–As angle (141.3 (2)°) is similar to the Ir–Sn–Ir angle (146.1 (1)°) and that, in both cases, the coordination about the silver or tin is planar.

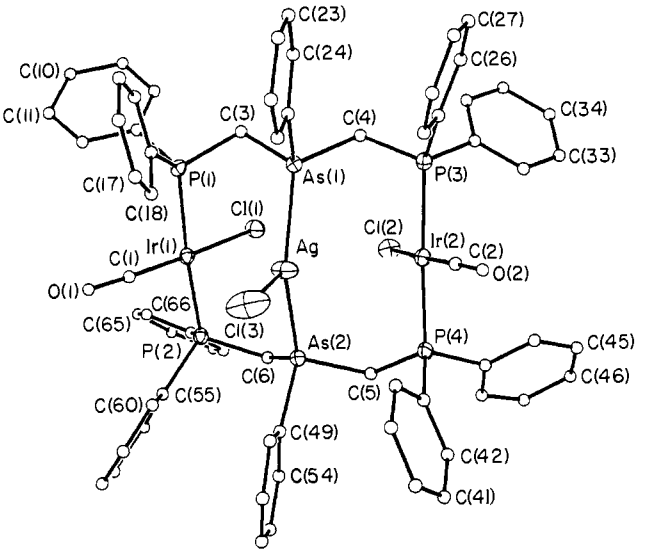

Figure 3. A perspective view of $Ir_2(AgCl)(CO)_2Cl_2(\mu\text{-dpma})_2$.

A perspective drawing of the anion, $Ir(SnCl_3)_2(CO)(dpma)]^-$, is shown in Figure 2. It has no crystallographically imposed symmetry. The five-coordinate iridium has trigonal bipyrimidal geometry with the P(6)IrC(67)O(3) unit comprising the axis. The P(6)Ir(3)C(67) angle, 178.8 (9)°, is nearly linear. The iridium ion is displaced very slightly out of the Sn_2P plane toward the carbonyl group. All of the P(6)–Ir(3)–equatorial ligand angles (range, 91.8–99.1°) are slightly greater than 90°, while the C(67)–Ir(3)–equatorial ligand angles (range, 81.7–87.2°) are less than 90°. Within the equatorial belt the Sn(2)–Ir(3)–Sn(3a) angle (108.7 (1)°) is compressed relative to the 120° ideal while the Sn(2)–Ir(3)–P(5) and the Sn(3A)–Ir(3)–P(5) angles (123.5 (2), 125.8 (2)) are expanded. The bond distances in this anion all appear quite normal. The dpma unit acts as bidentate ligand in which the arsenic atom is uncoordinated. Other examples of chelating dpma have been recently reported.[16]

Spectroscopic Studies. The tin adducts of **1** exhibit intense blue colors that make them sensitive detectors for tin. The electronic absorption spectrum of **3** shown in Figure 5 is dominated by an intense absorption at 588 nm. The spectrum of the corresponding $SnCl_3^-$ salt is nearly identical, while that of the sulfate complex **5** shows a slight but significant shift in λ_{max} to 582 nm.

These adducts are also luminescent in solution. Trace A of Figure 6 shows the emission spectrum of **3** in dichloromethane at 23 °C obtained upon excitation at 488 nm. Trace B shows the excitation spectrum recorded for emission at 645 nm. The excitation spectrum parallels the absorption spectrum shown in Figure 5. The small Stoke's shift observed for the emission and its near mirror image relation to the absorption at 588 nm suggests that this arises from a fluorescent process.

Metal Ion Replacement Reactions. The $SnCl^+$ unit is capable of replacing either Tl^+ or Pb^{2+} within the metallomacrocycle via the replacement reaction (eq 2). Trace A of Figure 6 shows the electronic absorption spectrum of an orange dichloromethane solution of $[Ir_2Tl(CO)_2Cl_2(\mu\text{-dpma})_2][NO_3]$.[8] Trace B shows the same sample after shaking with solid tin(II) chloride dihydrate. The solution is now blue. The absorption at 516 nm due to the thallium adduct has been replaced by a new absorption at 588

(13) Pelizzi, C.; Pelizzi, G.; Tarasconi, P. *J. Chem. Soc., Dalton Trans.* **1977**, 1935.
(14) Brady, R.; De Camp, W. H.; Flynn, B. R.; Schneider, M. L.; Scott, J. D.; Vaska, L.; Werneke, M. F. *Inorg. Chem.* **1975**, *14*, 2669.
(15) Wang, H.-H.; Pignolet, L. H.; Reedy, P. E., Jr.; Olmstead, M. M.; Balch, A. L. *Inorg. Chem.* **1987**, *26*, 377.
(16) Balch, A. L.; Olmstead, M. M.; Reedy, P. E., Jr.; Rowley, S. P. *Inorg. Chem.* **1988**, *27*, 4289.

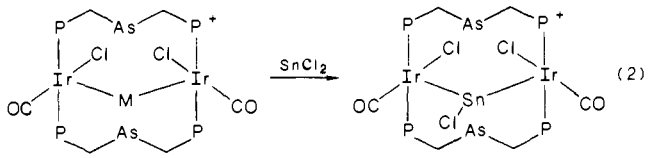

2a, M = Tl
b, M = Pb(NO_3)

nm that is characteristic of **3**. A similar reaction occurs with the lead adduct. Trace C of Figure 6 shows the spectrum of a pink dichloromethane solution of $[Ir_2Pb(CO)_2Cl_2(\mu\text{-dpma})_2][NO_3]_2$,[8] while Trace D shows the spectrum of the same solution after shaking with solid tin(II) chloride dihydrate. Further shaking with the tin(II) chloride results in complete loss of the band at 538 nm. The resulting blue solution shows the characteristic 588-nm absorption of **3**. This reaction is not quantitative; some loss of iridium complex presumably occurs because of absorption into the solid tin(II) chloride. Reversing the process, exposing dichloromethane solutions of **3** to solid thallium(I) nitrate or lead(II) nitrate, does not yield corresponding spectral changes. Similar replacement reactions occur when dichloromethane solutions of the lead and thallium complexes are treated with methanolic solutions of tin(II) chloride. We conclude that tin(II) is more strongly bound by **1** than is either thallium(I) or lead(II).

Extraction Studies. The iridium metallomacrocycle **1** in dichloromethane solution is capable of extracting tin(II) from an aqueous solution of tin(II) chloride. The electronic spectrum of 3.5 mL of a 0.68 mM dichloromethane solution of **1** that has been shaken with 2.0 mL of a 15 mM solution of tin(II) chloride dihydrate show 43% conversion of **1** to **3**. This process is unaffected by the presence of a variety of alkaline earth ions including Ba(II), Ca(II), and Sr(II). Sr(II) and Sn(II) have similar charges and ionic radii, so the extraction is chemoselective rather than size selective. We also find that mixing methanolic solutions of Ba(II), Ca(II), Sr(II), Na(I), K(I), Rb(I), and Cs(I) with dichloromethane solutions of **1** produce no electronic spectral changes. Thus even in a homogeneous reaction medium there is no uptake of these ions by **1**.

Transport Studies. The metallomacrocycle **1** is capable of transporting tin(II) from one aqueous solution through a dichloromethane solution (membrane) into a second aqueous phase. In a typical U-tube experiment[17] employing 5 mM dichloromethane solution of **1**, transport from an aqueous 15 mM solution of tin(II) chloride dihydrate yields detectable tin concentrations in the second phase after 3 days. During the process, the dichloromethane solution acquires the blue color characteristic of **3**, and the intensity of color of that solution remains stable for at least 4 days. The presence of Ca(II), Sr(II), or Rb(I) in the donor phase do not inhibit transport, nor are these ions transported. Under similar conditions, no transport of tin(II) was accomplished by 18-crown-6, which is capable of coordinating tin(II).[18] In fact, we are aware of no other studies demonstrating transfer of tin(II). Transport may be effected either through the reverse of reaction **1** or by the anion alone through the equilibrium shown in eq 3. We have not undertaken studies to differentiate between these possibilities.

$$SnCl_2 + Cl^- \rightleftharpoons SnCl_3^- \qquad (3)$$

Discussion

The metallomacrocycle **1** forms a tin(II) complex of unique structure and reactivity. Numerous transition-metal complexes of the $SnCl_3^-$ ion are known.[9] Only a few complexes with tin in different environments are known. Two are of particular relevance. The rhodium metallomacrocycle **6** binds 2 equiv of tin(II) chloride via reaction 4[19] One tin inserts into a Rh–Cl bond in an entirely normal fashion to become the terminal ligand on the right side

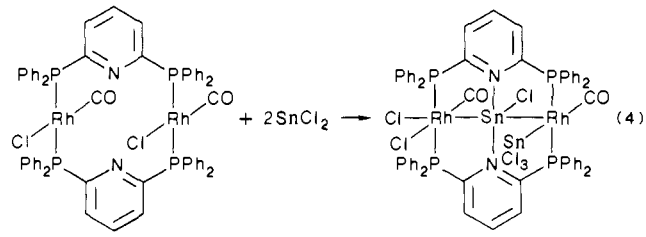

6 **7**

of **7**. The other inserts itself into the center of the metallomacrocycle, binds both rhodium ions, and oxidatively adds an Sn–Cl bond to one rhodium (the one on the left of **7**). Tin(II) chloride also reacts with 2 equiv of $(Me_3P)_3RhCl$ to form the unbridged molecule **8** in which the central tin has pseudotetra-

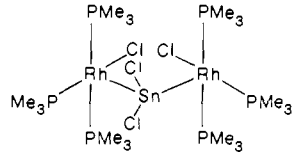

8

hedral Rh_2Cl_2 coordination.[20] Unlike the case of reaction **1**, both Sn–Cl bonds remain intact in this case. Thus there are important differences in the structure and bond present in each of the otherwise related complexes **3**, **7**, and **8**.

Kretschmer and Pregosin[21] have isolated a blue-green complex formulated as $IrCl(CO)(P(p\text{-}XC_6H_4)_3)_2SnCl_2$ (X = H, OCH_3, Cl, or F) (ν(CO), 2050, 1960 cm^{-1}) from the reaction of anhydrous tin(II) chloride with $IrCl(CO)(P(p\text{-}XC_6H_4)_3)_2$. They report that this material, unlike **3**, is very air sensitive. Under the conditions we used to prepared **3**, $Ir(CO)Cl(PPh_3)_2$ does not yield a blue- or green-colored complex. The difference in the infrared spectra of **3** and the Kretschmer/Pregosin complex suggests that they have different structures. Also note that the green complex, $Ir_2(SnCl_3)_2(CO)_2(\mu\text{-}S)(\mu\text{-dpm})_2$ (dpm is bis(diphenylphosphino)methane), formed by the reaction of tin(II) chloride with $Ir_2(\mu\text{-}S)(\mu\text{-dpm})_2$ in dichloromethane has a structure (involving an Ir–Ir bond with two terminal $SnCl_3^-$ ligands) that is quite different from that of **3**.[12]

We believe that the bonding in $[Ir_2(SnCl)(CO)_2Cl_2(\mu\text{-dpma})_2]^+$ involves interactions between the filled d_{z^2} orbitals on each iridium (that point toward the tin), the filled s orbital on tin, and the empty p_z orbitals on iridium and tin. The simple molecular orbital diagram for a nearly linear MM'M system which we have used elsewhere to account for the bonding in nearly linear chains with $(d^8d^8d^8)$,[3,22] $(d^8d^{10}d^8)$,[7] $(d^8s^2d^8)$,[8] and $(s^2d^8s^2)$[23] electronic configurations for each of the three metal ions can be adapted to account for the bonding in **2** and **3**. That scheme is shown in Figure 8, where interaction of the filled $5d_{z^2}$ orbitals on iridium and the filled 5s orbital on tin produces a filled set of orbitals ($1a_1$, $1b_2$, and $2a_1$), while interaction of the three empty p_z orbitals produces a set of empty orbitals ($2b_2$, $3a_1$, $3b_2$). Mixing of orbitals of like symmetry in the filled and empty sets yields net stabilization of the filled orbitals. The intense electronic transition responsible for the blue color of $[Ir_2(SnCl)(CO)_2Cl_2(\mu\text{-dpma})_2]^+$ is assigned as a transition from the filled $d^8s^2d^8$ to an empty ppp molecular orbital ($2a_1 \rightarrow 2b_2$ transition in Figure 8).

Experimental Section

Materials. $Ir_2(CO)_2Cl_2(\mu\text{-dpma})_2$,[2] **1**, $Ir_2(CO)_2Cl_2(\mu\text{-dppp})_2$,[15] $[Ir_2Tl(CO)_2Cl_2(\mu\text{-dpma})_2][NO_3]$,[8] and $[Ir_2Pb(CO)_2Cl_2(\mu\text{-dpma})_2][NO_3]_2$[8] were prepared as previously described. No special precautions were used to exclude oxygen or moisture during the synthesis of the complexes.

(17) Fyles, T. M. *J. Chem. Soc., Faraday Trans. 1* **1986**, *82*, 617 and references therein.
(18) Herber, H. R.; Smelkinson, A. E. *Inorg. Chem.* **1978**, *17*, 1023.
(19) Balch, A. L.; Hope, H.; Wood, F. E. *J. Am. Chem. Soc.* **1985**, *107*, 6936.
(20) Chan, D. M. T.; Marder, T. B. *Angew. Chem., Int. Ed. Engl.* **1988**, *27*, 442.
(21) Kretschmer, M.; Pregosin, P. S. *Inorg. Chim. Acta* **1982**, *61*, 247.
(22) Balch, A. L.; Fossett, L. A.; Nagle, J. K.; Olmstead, M. M. *J. Am. Chem. Soc.* **1988**, *110*, 6732.
(23) Nagle, J. K.; Balch, A. L.; Olmstead, M. M. *J. Am. Chem. Soc.* **1988**, *110*, 319.

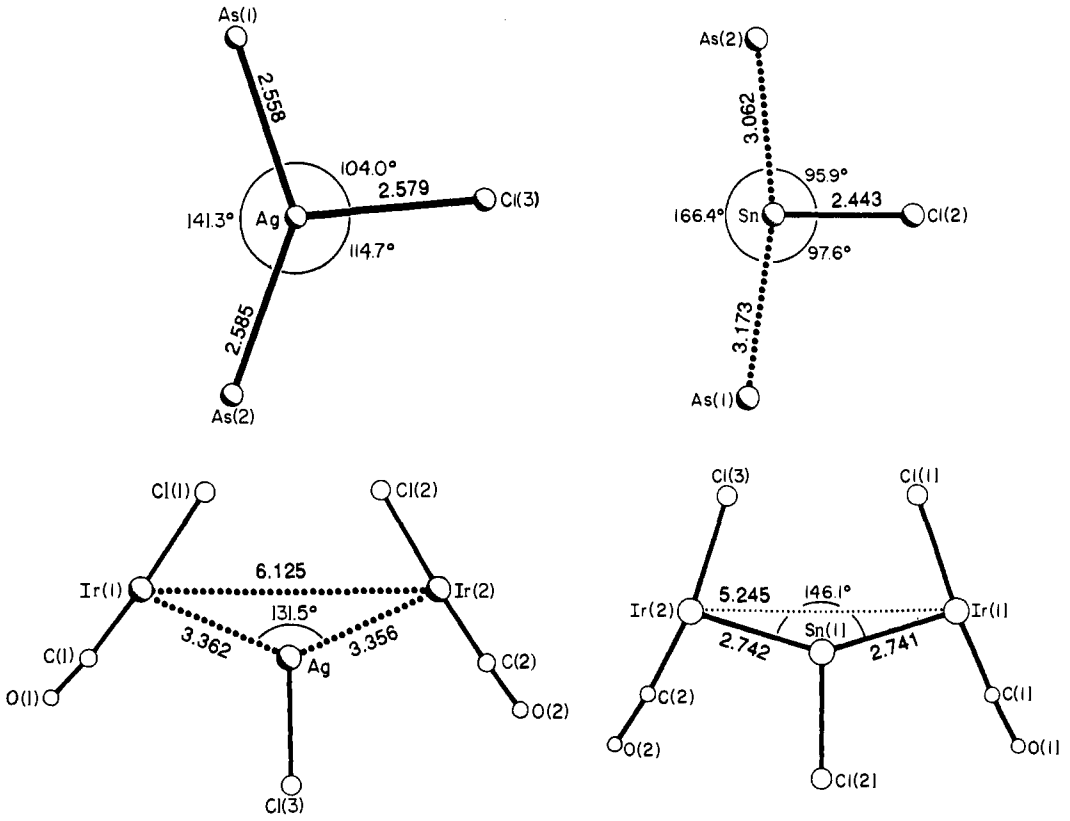

Figure 4. Comparisons of the central metal binding sites in left, $Ir_2(AgCl)(CO)_2Cl_2(\mu\text{-dpma})_2$, and right, $[Ir_2(SnCl)(CO)_2Cl_2(\mu\text{-dpma})_2]^+$.

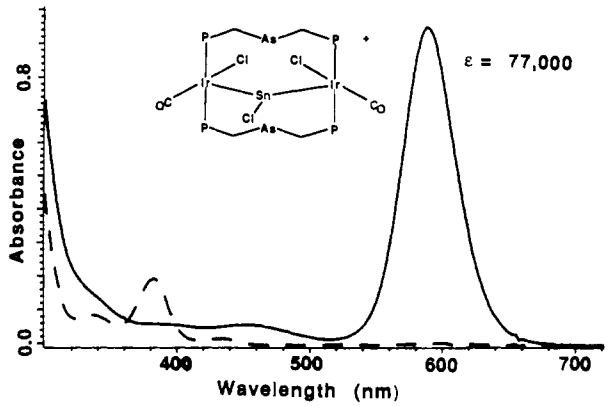

Figure 5. Solid line: electronic absorption spectrum of $[Ir_2(SnCl)(CO)_2Cl_2(\mu\text{-dpma})_2][BPh_4]$ in dichloromethane solution. Broken line: corresponding spectrum for $Ir_2(CO)_2Cl_2(\mu\text{-dpma})_2$.

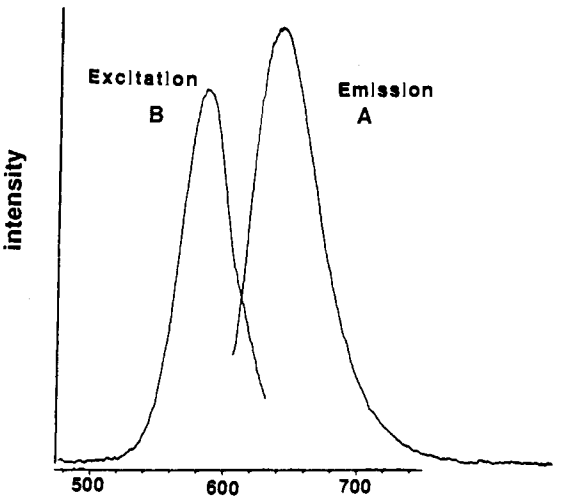

Figure 6. A, emission spectrum from **3** in dichloromethane with excitation at 588 nm. B, excitation spectrum of **3** for emission at 645 nm.

Preparation of Compounds. **$[Ir_2(SnCl)(CO)_2Cl_2(\mu\text{-dpma})_2][SnCl_3]$, 3.** A solution of 100 mg (0.44 mmol) of $SnCl_2{\cdot}2H_2O$ dissolved in 2 mL of methanol was added to a solution of 100 mg (0.062 mmol) of $Ir_2(CO)_2Cl_2(\mu\text{-dpma})_2$ in 4 mL of dichloromethane. The solution immediately turned deep blue in color. After stirring for 5 min, an additional 5 mL of methanol was added slowly, causing the product to precipitate as blue needles. The product was collected by filtration and washed successively with methanol and diethyl ether: yield 110 mg, 89%. Infrared (Nujol) ν(CO) 1987, 1974 cm^{-1}; ^{31}P NMR δ 26.9 ppm; conductivity, Λ_M = 49 ohm^{-1} mol^{-1} cm^2; UV–vis $\lambda_{max}(\epsilon)$ 588 nm (77 000), 450 (4800), 399 (4100), 311 (18 000). Anal. Calcd for $C_{66}H_{58}As_2Cl_6Ir_2O_2P_4Sn_2$: C, 39.81; H, 2.94; Cl, 10.68. Found: C, 38.81; H, 2.87; Cl, 10.97.

$[Ir_2(SnCl)(CO)_2Cl_2(\mu\text{-dpma})_2][BPh_4]$, 4. This complex was prepared by dissolving 100 mg (0.05 mmol) of **3** in a minimum amount of dichloromethane and adding to this a solution of 100 mg (0.29 mmol) of sodium tetraphenylborate dissolved in 2 mL of methanol. Addition of 5 mL of methanol caused the product to precipitate as blue needles. The product was collected by filtration and washed successively with methanol and diethyl ether: yield 98 mg, 94%. Infrared (Nujol) ν(CO) 1983, 1977 cm^{-1}; ^{31}P NMR δ 26.9 ppm; conductivity (dichloromethane solution) Λ_M = 52 ohm^{-1} mol^{-1} cm^2; UV–vis (dichloromethane) 566 nm (73 000), 452 (4800), 399 (4100), 311 (16 000). Anal. Calcd for $C_{90}H_{78}As_2BCl_3Ir_2O_2P_4Sn$: C, 51.84; H, 3.77; Cl, 5.10. Found: C, 51.34; H, 3.70; Cl, 5.35.

$Ir_2(SnSO_4)(CO)_2Cl_2(\mu\text{-dpma})_2{\cdot}0.2CH_2Cl_2$, 5. A slurry of 100 mg (0.47 mmol) of $SnSO_4$ in 0.25 mL of water and 2 mL of methanol was added to a solution of 100 mg (0.062 mmol) of $Ir_2(CO)_2Cl_2(\mu\text{-dpma})_2$ in 4 mL of dichloromethane. The mixture was stirred for 20 mins, at which time the deep blue solution was filtered to remove unreacted $SnSO_4$. Addition of 5 mL of methanol caused the product to precipitate as blue crystals. The product was collected by filtration and washed successively with methanol and diethyl ether: yield 85 mg, 75%. The presence of dichloromethane was confirmed by ^1H NMR. Infrared (Nujol) ν(CO) 1991; ^{31}P NMR δ 22.4 ppm. Conductivity (dichloromethane solution) Λ_M = 0 ohm^{-1} mol^{-1} cm^2; UV–vis (dichloromethane solution) λ_{max} (ϵ), 582 (99 000), 371 (8100), 310, (12 000), 296 (13 000). Anal. Calcd for $C_{66.2}H_{58.4}As_2Cl_{2.4}Ir_2O_6P_4SSn$: C, 43.09; H, 3.19; Cl, 4.69. Found: C, 42.95; H, 3.21; Cl, 4.69.

$Ir_2(AgCl)(CO)_2Cl_2(\mu\text{-dpma})_2$. Dichloromethane (5 mL) was added to a mixture of 50 mg (0.031 mmol) of $Ir_2(CO)_2Cl_2(\mu\text{-dpma})$ and 50 mg

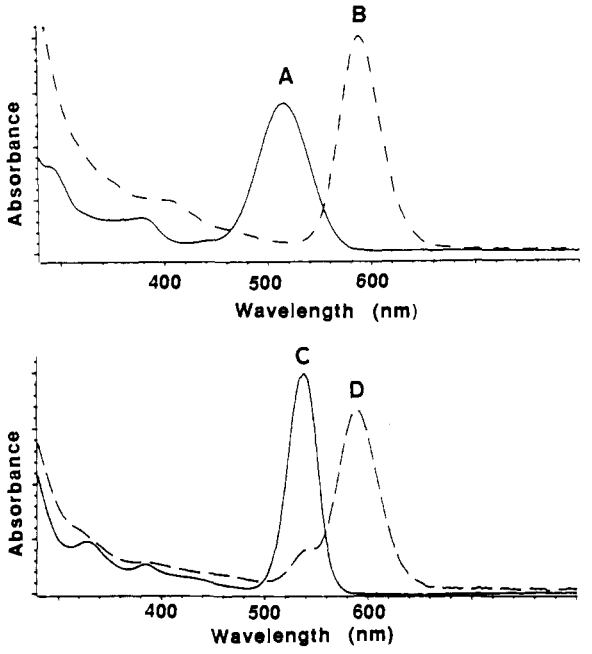

Figure 7. A, electronic absorption spectrum of a dichloromethane solution of $[Ir_2Tl(CO)_2Cl_2(\mu\text{-dpma})_2][NO_3]$. B, the same solution after shaking with solid tin(II) chloride dihydrate. C, electronic absorption spectrum of $[Ir_2Pb(CO)_2Cl_2(\mu\text{-dpma})_2][NO_3]_2$. D, the same solution after shaking with solid tin(II) chloride dihydrate.

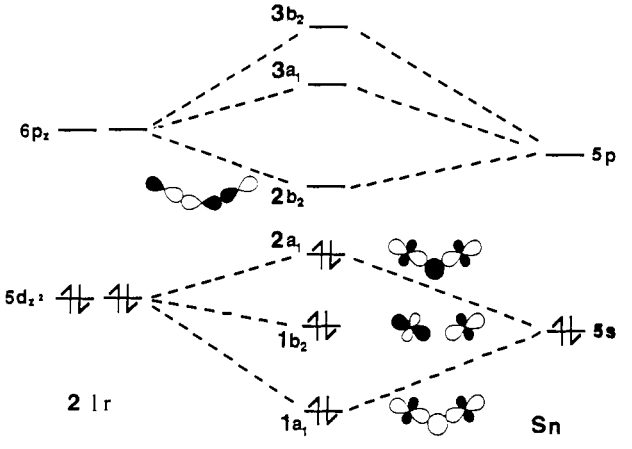

Figure 8. A qualitative molecular orbital scheme for **3** showing the important interactions within the Ir–Sn–Ir unit.

(0.34 mmol) of silver chloride. The mixture was stirred overnight to give a golden solution and a yellow solid. The solution was filtered, and the solid was washed with five 2-mL portions of dichloromethane so that only white, unreacted silver chloride remained on the filter. Diethyl ether was added gradually to the combined yellow filtrate to give yellow crystals of the product [yield 48 mg, 86%; infrared (Nujol) ν(CO) 1957 cm^{-1}; ^{31}P NMR δ 20.9 ppm]. Suitable crystals for X-ray crystallography were grown by diffusion of diethyl ether into a dichloromethane solution of the complex. $Ir_2(AgCl)(CO)_2Cl_2(\mu\text{-dpma})_2\cdot 1.8\ CH_2Cl_2$ crystallizes in the triclinic space group $P\bar{1}$ (no. 2) with a = 10.974 (5) Å, b = 15.042 (5) Å, c = 21.710 (8) Å, α = 94.97 (3), β = 101.72 (3), γ = 93.67 (3) at 130 K. Least-squares refinement of 419 parameters using 8397 reflections yield R = 0.048, R_w = 0.054.

Physical Measurements. The ^{31}P NMR spectra were recorded with proton decoupling on a Nicolet NT-200 Fourier transform spectrometer operating at 81 MHz, with an external 85% phosphoric acid standard. The high frequency positive convention, recommended by IUPAC, has been used in reporting all chemical shifts. Infrared spectra were recorded from mineral oil mulls with an IBM IR32 infrared spectrometer. Electronic absorption spectra were recorded on a Hewlett-Packard 8450A spectrometer. Emission spectra were recorded on a Perkin-Elmer MPF-44B fluorescence spectrophotometer.

X-ray Data Collection. Solution and Refinement for $[Ir_2(SnCl)(CO)_2Cl_2(\mu\text{-dpma})_2][Ir(SnCl_3)_2(CO)(dpma)]\cdot 2.25CH_2Cl_2$. Due to the difficulty in obtaining suitable crystals of either the $SnCl_3^-$ or BPh_4^- salts

Table IV. Crystal Data and Data Collection Parameters[a] for $[Ir_2(SnCl)(CO)_2Cl_2(\mu\text{-dpma})_2][Ir(CO)(SnCl_3)_2(dpma)]\cdot 2.5CH_2Cl_2$

formula	$Ir_3Sn_3As_3Cl_{13.5}P_6O_3C_{101.25}H_{85.5}$
fw	3172.21
crystal system	triclinic
space group	$P\bar{1}$ (no. 2)
cryst dimens, mm	0.12 × 0.37 × 0.37
color and habit	red/green parallelepipeds
unit cell dimens (130 K)	
a, Å	16.739 (7)
b, Å	17.030 (7)
c, Å	21.785 (9)
α, (deg)	79.61 (3)
β, (deg)	75.97 (3)
γ, (deg)	67.78 (3)
V, Å^3	5550 (3)
$D_{(calcd\ 130\ K)}$, g/cm^3	1.90
Z	2
radiation, λ, Å (graphite monochromator)	Mo Kα, 0.71069
μ(Mo Kα) cm^{-1}	58.0
transmission factors	0.16–0.55
octants	$+h,\pm k,\pm l$
scan type, 2θ max (deg)	ω, 45
scan range (deg)	1.4
scan speed (deg min^{-1})	15
check refl, interval no.	2, 198
no. of unique data	14429
no. data $I > 3\sigma I$	7363
params refined	665
R^b	0.063
R_w^c	0.063

[a] Diffractometer: Syntex $P2_1$. [b] $R = \sum||F_o| - |F_c||/|F_o|$. [c] $R_w = \sum||F_o| - |F_c||w^{1/2}/\sum|F_o|w^{1/2}$; $w = [\sigma^2|F_o|]^{-1}$.

3 and **4**, the following procedure was used. A methanol solution containing tin(II) chloride dihydrate and sodium tetraphenylborate was allowed to diffuse slowly into a dichloromethane solution of $Ir_2(CO)_2Cl_2(\mu\text{-dpma})_2$, **1**. Initially only small, blue/green needles grew, but after 6 weeks large, well-formed parallelepipeds had formed. The crystals were coated with a hydrocarbon oil to retard loss of solvent dichloromethane, but the cracking that occurred in a few moments and the partial occupancy of dichloromethane in the structure indicate that these crystals readily lose dichloromethane of crystallization. A suitable crystal was mounted on a glass fiber with silicone grease and positioned in the cold stream of the diffractometer with the long dimension of the crystal parallel to ϕ. No decay in the intensities of three standard reflections was observed during the course of the data collection. Crystal data are given in Table IV.

The usual corrections for Lorentz and polarization effects were applied to the data. Crystallographic programs used were those of SHELXTL, version 4, installed on a Data General Eclipse computer. Scattering factors and corrections for anomalous dispersion were from the "International Tables", Vol. IV.[24]

Solution of the structure was accomplished by Patterson methods. An absorption correction was applied.[25] One low-angle reflection that was affected by extinction was removed from the data. One of the three molecules of dichloromethane is disordered around a center of symmetry and is only partially present. Its chlorine atom was arbitrarily assigned an occupancy of 0.5. The bonded carbon was not located. In the anion one of the $SnCl_3$ groups is ordered, but the other is disordered in sets "A" and "B" with refined group occupancies of 0.618 (4) and 0.382 (4), respectively. One of the chlorines in set B is present in two approximately equal sites as well; these chlorines are labeled Cl(9B) and Cl(9C). In the final cycles of refinement Ir, As, P and the nondisordered Sn and Cl atoms were assigned anisotropic thermal parameters. In the final difference map the largest feature was 2.6 e Å^{-3} in height, in the vicinity of one of the arsenics. There were several other spurious features in the vicinity of the heavy atoms, probably due to the large absorption effects of this crystal.

Acknowledgment. We thank the National Science Foundation (CHE 8519557) for support, Johnson Matthey Inc. for a loan of iridium, Dow Corning Corp. for a fellowship for P.E.R., and the

(24) *International Tables for X-ray Crystallography*; Kynoch Press: Birmingham, England, 1974; Vol. IV., pp 149–150, 99–101.

(25) XABS produces an absorption tensor from an expression relating F_o and F_c. Moezzi, B. Ph.D. Thesis, University of California, Davis, CA, 1988.

Earle C. Anthony Fund for a fellowship for D.E.O.

Supplementary Material Available: Tables of bond distances, angles, and anisotropic thermal parameters for $[Ir_2(SnCl)(CO)_2Cl_2(\mu\text{-dpma})_2][Ir(SnCl_3)_2CO(dpma)]\cdot 2.25CH_2Cl_2$, tables of atomic positional parameters, bond distances, angles, anisotropic thermal parameters, and hydrogen positions for $[Ir_2(AgCl)(CO)_2Cl_2(\mu\text{-dpma})_2]\cdot 1.8CH_2Cl_2$, and full details of data collection, solution, and refinement (18 pages). Ordering information is given on any current masthead page.

Enantioselective Addition of Dialkylzincs to Aldehydes Promoted by Chiral Amino Alcohols. Mechanism and Nonlinear Effect

M. Kitamura, S. Okada, S. Suga, and R. Noyori*

Contribution from the Department of Chemistry, Nagoya University, Chikusa, Nagoya 464, Japan. *Received September 2, 1988*

Abstract: In the presence of a catalytic amount of (−)-3-*exo*-(dimethylamino)isoborneol (DAIB), reaction of dialkylzincs and aldehydes is accelerated markedly to give, after hydrolysis, the corresponding *S*-alcohols in high enantiomeric purity. The reaction mechanism and origin of the enantioselection have been elucidated on the basis of the kinetic measurement, alkyl-scrambling experiments, single-crystal X-ray analysis, ^1H NMR study, molecular weight determination of certain key intermediates. Reaction of DAIB and dimethylzinc in a 1:1 molar ratio produces a single dinuclear zinc chelate complex, which does not alkylate benzaldehyde but acts as catalyst precursor. The alkylation proceeds via a dinuclear zinc species containing the DAIB auxiliary, an aldehyde ligand, and three alkyl groups, where it is the bridging alkyl group, rather than the terminal alkyls, that migrates from zinc to the aldehyde carbon. Kinetic measurements and temperature effects on the enantioselectivity indicate that the alkyl transfer process is the turnover-limiting and stereodetermining step. A new type of nonlinear effect has been observed in this enantioselective alkylation. For example, reaction of benzaldehyde and diethylzinc in the presence of 8 mol % of (−)-DAIB in 15% ee leads to (*S*)-1-phenyl-1-propanol in 95% ee. This unusual phenomenon is a result of a marked difference in chemical properties of the diasteromeric dinuclear complexes formed from dialkylzincs and the DAIB auxiliary. Reaction of equimolar amounts of dimethylzinc and enantiomerically pure DAIB affords a dinuclear chelate complex with C_2 chirality, which acts as the active catalyst precursor of the alkylation. By contrast, dimethylzinc and racemic DAIB generate a more stable, but much less reactive, dinuclear complex possessing a meso, C_i structure, rather than a racemic mixture of the chiral complex.

Monomeric dialkylzincs having an sp hybridized, linear geometry are inert to simple carbonyl compounds, because the alkyl–metal bond is rather nonpolar. However, addition of certain donor ligands or auxiliaries can generate coordinatively unsaturated, bent structures possessing higher reactivity. Particularly, replacement of the alkyl group by an electronegative substituents increases polarity of the alkyl–Zn bond to a great extent and, consequently, enhancement of the donor property of the alkyl group and the acceptor character of the Zn atom is the result.[1] In 1986, we

reported that dialkylzincs react with aldehydes in the presence of a catalytic amount of (−)-3-*exo*-(dimethylamino)isoborneol (DAIB) to give after hydrolysis the corresponding *S*-alcohols in high (up to 99%) enantiomeric purities.[2,3] The sterically con-

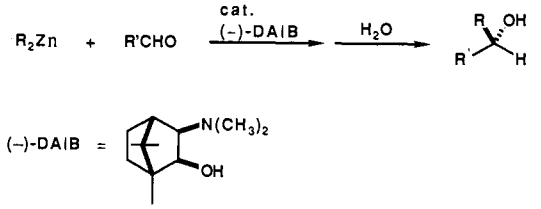

strained β-dialkylamino alcohol not only accelerates the alkylation reaction but also directs the stereochemical outcome in the absolute sense. Various para-substituted benzaldehydes give consistently high enantioselectivity, suggesting that the stereoselection is steric

Table I. Effect of the C_6H_5CHO:$(C_2H_5)_2Zn$:(−)-DAIB Molar Ratio on Reactivity[a]

ratio			(*S*)-1-phenyl-1-propanol	
C_6H_5CHO	$(C_2H_5)_2Zn$	(−)-DAIB	% yield[b]	% ee[c]
1	1	0	0[d]	
1	1	1	1[e]	0
1	2	2	0[f]	
1	2	1	88[d]	98
2	2	1	49[g]	96
100	50	1	48[h]	98
50	50	1	97[d]	98

[a] All reactions were carried out under argon at 0 °C in degassed anhydrous toluene unless otherwise specified. [b] HPLC analysis (Develosil 100-5, ether–hexane). Based on benzaldehyde. [c] HPLC analysis (Bakerbond DNBPG covalent type, 2-propanol–hexane). [d] Benzyl alcohol was obtained in 1–3% yield. [e] After 170 h, 29% of benzyl alcohol was obtained. [f] After 1500 h, 64% of benzyl alcohol was obtained. [g] After 170 h, 13% of benzyl alcohol was obtained. [h] After 170 h, 12% of benzyl alcohol and 10% of propiophenone were obtained.

(1) Boersma, J. In *Comprehensive Organometallic Chemistry*; Wilkinson, G., Ed.; Pergamon Press: New York, 1982; Chapter 16.
(2) Kitamura, M.; Suga, S.; Kawai, K.; Noyori, R. *J. Am. Chem. Soc.* **1986**, *108*, 6071.
(3) For related reactions, see: (a) Oguni, N.; Omi, T. *Tetrahedron Lett.* **1984**, *25*, 2823. (b) Smaardijk, A. A.; Wynberg, H. *J. Org. Chem.* **1987**, *52*, 135. (c) Itsuno, S.; Fréchet, J. M. J. *J. Org. Chem.* **1987**, *52*, 4140. (d) Soai, K.; Ookawa, A.; Ogawa, K.; Kaba, T. *J. Chem. Soc., Chem. Commun.* **1987** 467. Soai, K.; Ookawa, A.; Kaba, T.; Ogawa, K. *J. Am. Chem. Soc.* **1987**, *109*, 7111. (e) Chaloner, P. A.; Perera, S. A. R. *Tetrahedron Lett.* **1987**, *28*, 3013. (f) Corey, E. J.; Hannon, F. J. *Tetrahedron Lett.* **1987**, *28*, 5233. (g) Corey, E. J.; Hannon, F. J. *Tetrahedron Lett.* **1987**, *28*, 5237. (h) Evans, D. A. *Science* **1988**, *240*, 420.

0002-7863/89/1511-4028$01.50/0